Decomposition and Inference of Sources through Spatiotemporal Analysis of Network Signals: The DISSTANS Python Package

Tobias Köhne[1], Bryan Riel[2], and Mark Simons[1]

[1]California Institute of Technology
[2]Massachusetts Institute of Technology

November 21, 2022

Abstract

Regional-scale, continuously-operating Global Navigation Satellite System (GNSS) networks are a powerful tool to monitor plate motion and surface deformation. Since their inception, their size, density, and length of observation record have steadily increased throughout the world. Simultaneously, researchers have had to write accompanying software to enable the analysis (especially the decomposition) of the ever-increasing amount of available timeseries in an efficient way. These codes and respective studies have individually set standards for different subsets of the following desirable qualities: portability (between locations), speed (code runtime), automation (avoiding or simplifying manual inspection of each station), use of spatial correlation (exploiting the fact that stations experience common signals), availability (open source), and documentation (of the usage and underlying methods). In this study, we present the DISSTANS Python package, which aims to combine the aforementioned achievements in a single software by offering generic (therefore portable), parallelizable (fast) methods that can exploit the spatial structure of the observation records in a user-assisted, semi-automated framework, including uncertainty propagation. The code is open source, includes an application interface documentation as well as usage tutorials, is easily extendable, and is based on the previously published and validated method of Riel et al. (2014). We also present two case studies to validate our code, one using a synthetic dataset and one using real GNSS network timeseries.

Decomposition and Inference of Sources through Spatiotemporal Analysis of Network Signals: The DISSTANS Python Package

Tobias Köhne[1], Bryan V. Riel[2], Mark Simons[1]

[1] Seismological Laboratory, Division of Geological and Planetary Sciences, California Institute of Technology; [2] Department of Earth, Atmospheric and Planetary Sciences, Massachusetts Institute of Technology

DISSTANS

Check out the GitHub repository for the code and documentation!

github.com/tobiscode/disstans

tkoehne@caltech.edu

www.tobiaskoehne.de

AGU Fall Meeting 2021 T45D-0264

I. DISSTANS At A Glance

- **Decompose timeseries** into parameterized, function-defined models (from simple polynomials to magnitude-varying sinusoids and dictionaries of transient splines)
- Designed for **Global Navigation Satellite Systems (GNSS) networks of position timeseries**, but easily adaptable for other timeseries
- Solve for parameters with **least squares** and **L2, L1 and L0 regularization norms**
- Include **spatial awareness** in the estimate of model parameters using **spatial L0-regularization** (Riel et al., 2014)
- Take advantage of CPU-based **parallelization** (with GPU capabilities planned)
- Create **maps and visualizations** with simple commands
- **Open-source code**, full online documentation
- Create synthetic timeseries, manage RINEX databases, incorporate maintenance and seismic catalogs, detect data jumps, and much more

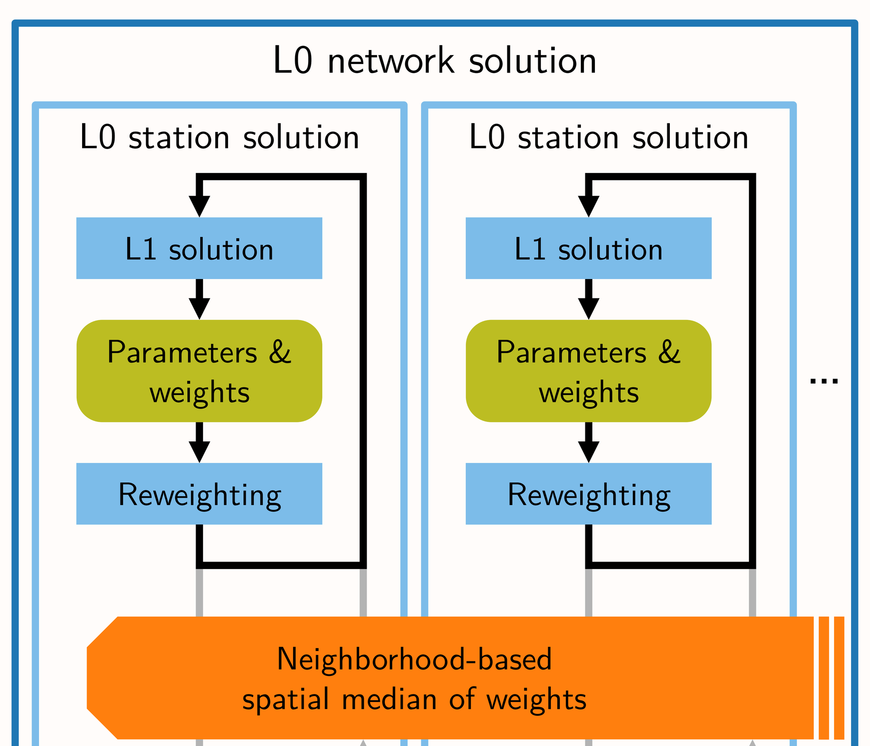

Spatial L0 regularization

- **Sparsity** is important for geophysical inverse problems that focus on the **detection of signals**.
- L1 and L0 norms penalize the **magnitude and existence of parameters**, respectively, for a **single** timeseries (i.e., locally).
- **Spatial L0** extends the regularization to **promote signals that are coherently present in space**, while penalizing parameters that are only seen at isolated locations (Riel et al., 2014).

Fig. 1: Visualization of the implementation of the sparsity-promoting regularization schemes in DISSTANS. The L1 solution is computed using CVXPY (Agrawal et al., 2018; Diamond & Boyd, 2016). By reweighting the parameter-specific penalties and iterating, the L1 solution converges to the (local) L0 solution (Candès et al., 2008). Combining the reweighted penalties across the network then yields the spatial L0 solution (Riel et al., 2014).

II. Validation: Synthetic GNSS Networks

The timeseries for all synthetic networks were created using tools included in DISSTANS.

Transient signal extraction performance as a function of network size and noise level

Using a large number of different network geometries and relative noise levels, we find that DISSTANS is able to:

- **Decrease the average error** (misfit between model and truth) over the stations in the network.
- **Decrease the error variance** of the fit between sampled networks.

These reductions highlight DISSTANS' potential to identify processes with low signal-to-noise ratio.

Fig. 2 (right): Average errors of synthetic networks of varying sizes and geometries for different relative noise levels σ (colored lines). Every station is affected by the same transient displacement signal. The sample mean over all simulated networks of the average error within each network is on the vertical axis, and the number of stations used is on the horizontal axis. Errorbars are the sample standard deviation over all simulated networks of the average error. The dashed line is the theoretical error if the regularization would prevent any signal to be fitted. The dotted line is a reference line proportional to the inverse square root of the number of stations.

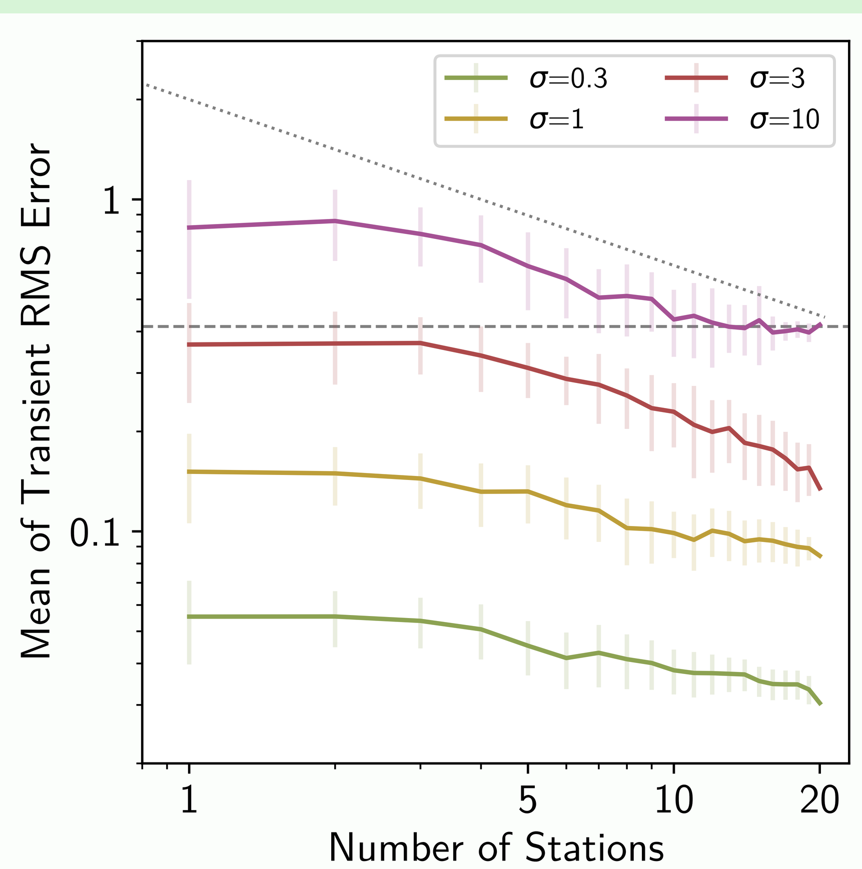

Benefits of using spatial L0 regularization in a synthetic network affected by multiple signals

- DISSTANS **better recovers** the **true direction and amplitude** of motion when going from local to spatial L0 regularization.
- Improvements are present in both **high and low signal-to-noise-ratio** timeseries (also see Fig. 2).

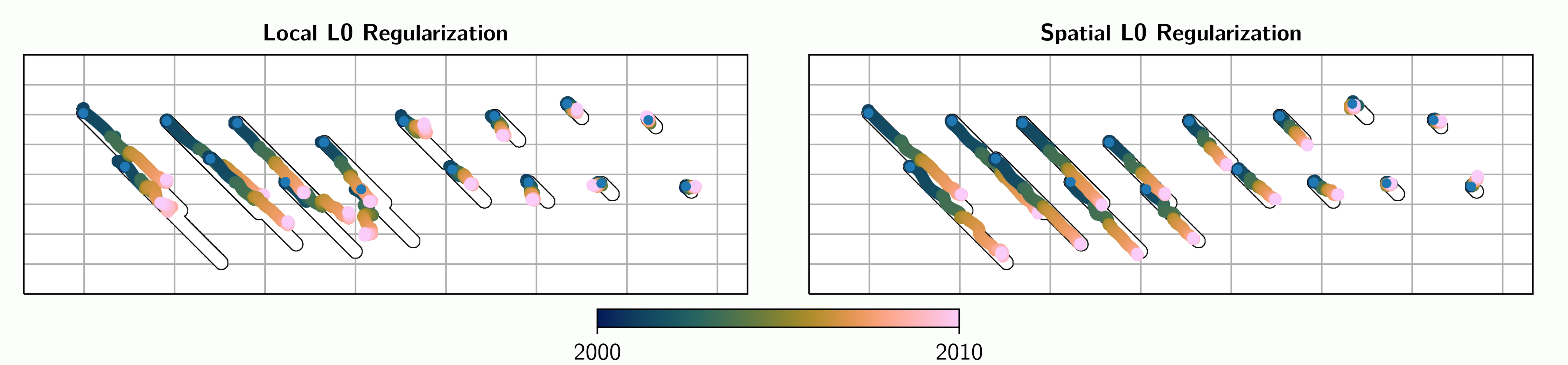

Fig. 3: Map view of the extracted transient motion of a synthetic network analyzed with local and spatial L0 regularization. The colored curves track the location of a station relative to its initial position, with the colors corresponding to time. The true transient is shown by the black outlines. The network is also affected by secular, annual, biannual, coseismic and postseismic motion, as well as Gaussian noise.

III. Validation: Long Valley Caldera, California, USA

Raw GNSS timeseries for the Long Valley Caldera and surrounding regions were downloaded from the University of Nevada at Reno's Nevada Geodetic Laboratory (Blewitt et al., 2018).

Study location

We choose data from the Long Valley Caldera (LVC) region to validate our code because:

- It is affected by **multiple significant processes**, e.g., episodic, aseismic **transient motion**, and significant, **time-varying seasonal hydrological loading.**
- The **long displacement timeseries** from the local GNSS network has been extensively studied by others (e.g., Ji et al., 2013; Montgomery-Brown et al., 2015; Silverii et al., 2020).

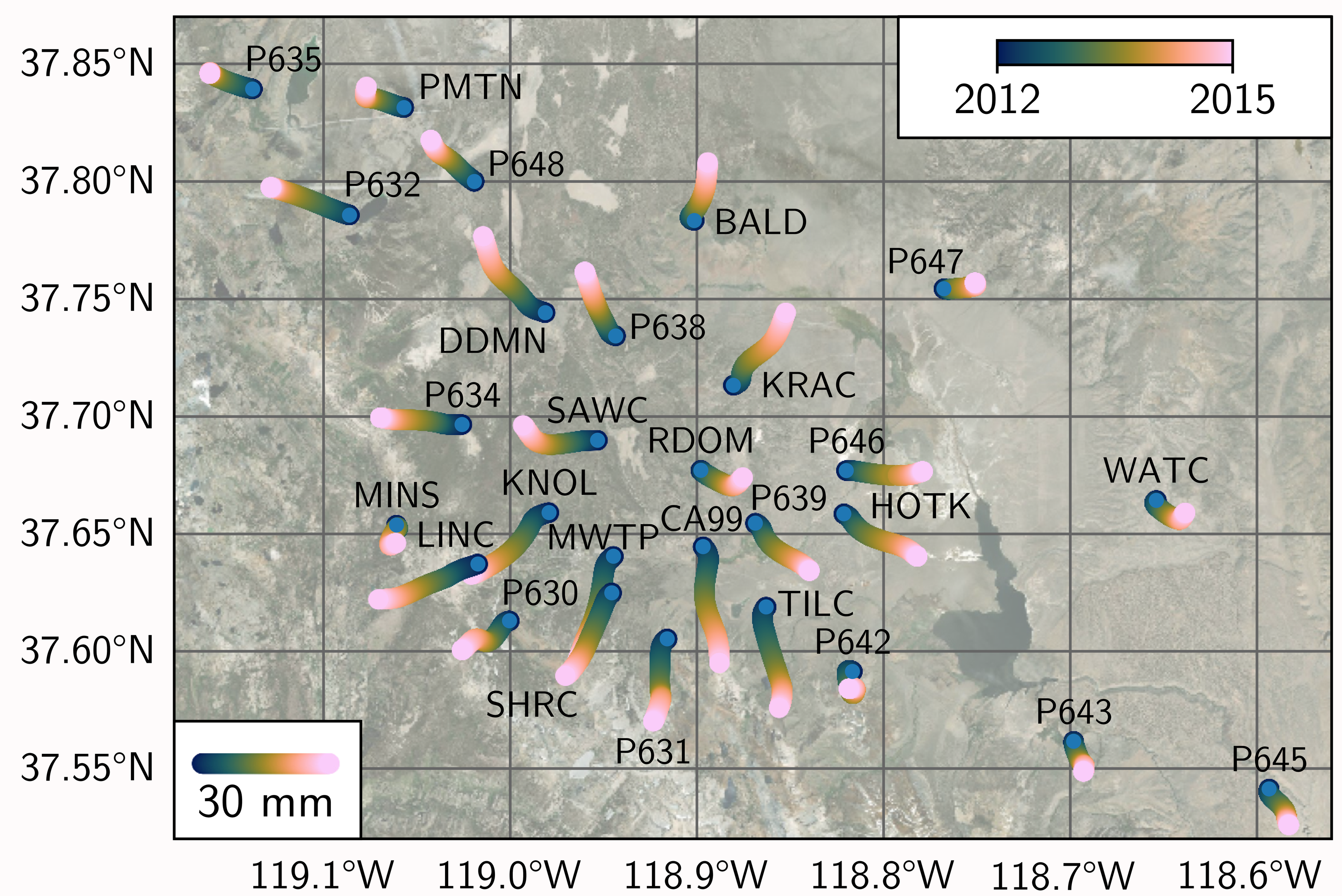

Fig. 4: Modeled horizontal transient displacements of selected stations inside the Long Valley Caldera during the period between 2012 and 2015. The curves track the location of a station relative to its initial position, with their colors corresponding to time. Outward horizontal motion during the period of rapid extension is clearly visible (compare Ji et al., 2013; Montgomery-Brown et al., 2015). Background satellite imagery by Earthstar Geographics & Esri.

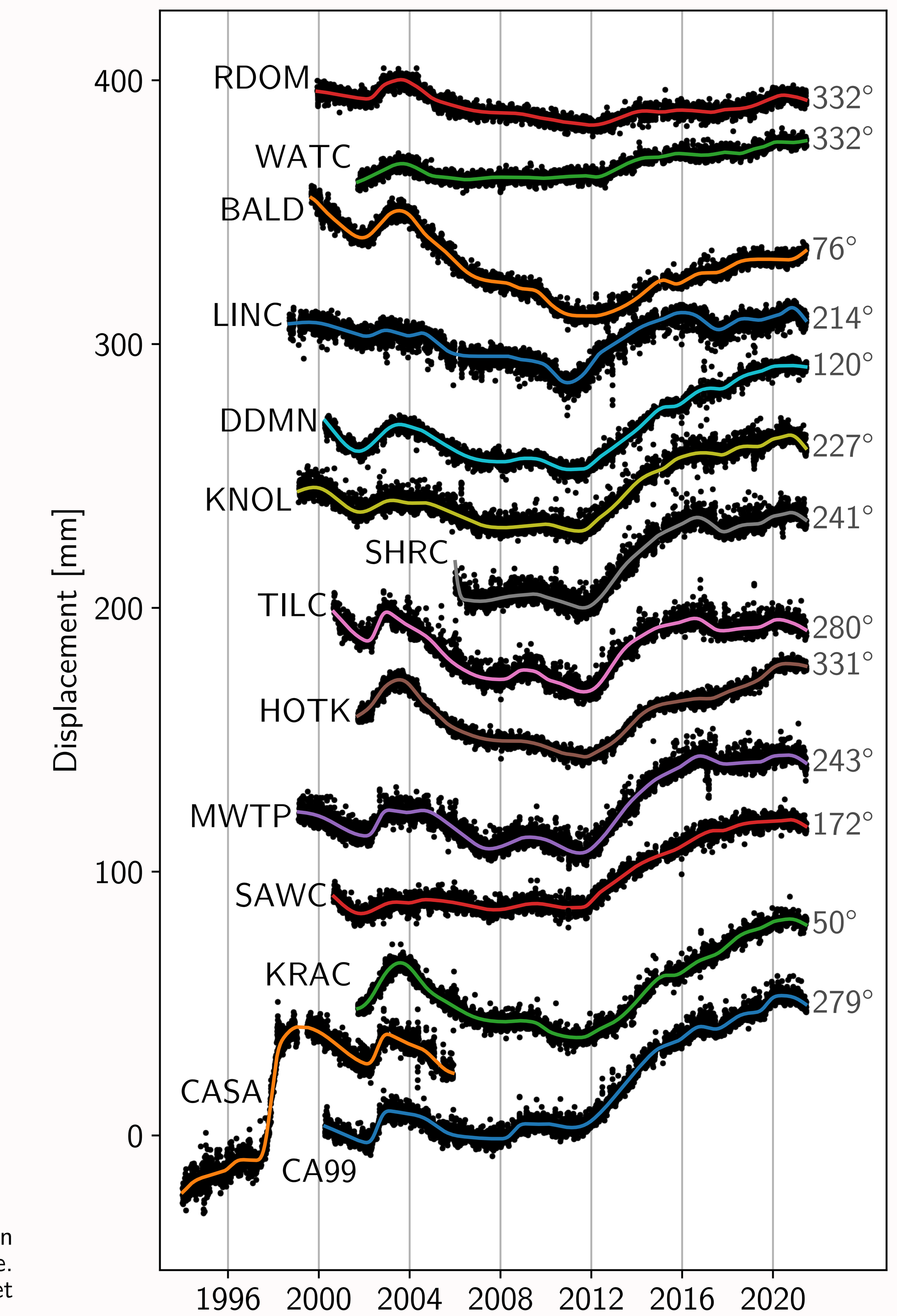

Fig. 5 (left): Modeled horizontal transient displacement (colored lines) of selected stations (names on the left) from Fig. 4, projected along the direction of maximum displacement during the period between 2012 and 2015. The directions (in grey to the right) are measured counterclockwise from east. CA99's direction is used for CASA. Black dots are the joint model's residuals, centered on the transient model. The transient motions clearly exhibit spatiotemporally coherent periods of expansion (compare Silverii et al., 2020).

Horizontal transient motion

- Transient motion is modeled with an **overcomplete dictionary of integrated cardinal B-splines** of varying periods (tens to hundreds of days) and center times (thousands of elements in total).
- Sparsity is promoted in space and time with **spatial L0 regularization**.
- **No assumption** about a steady-state velocity is made.

Variable-amplitude vertical seasonal signal

The seasonal signal for each frequency and data component is modeled as $(\bar{a} + a(t)) \cdot \cos(\omega t) + (\bar{b} + b(t)) \cdot \sin(\omega t)$, where:

- $\bar{a}$ and $\bar{b}$ are constant and **unregularized**, forming the **nominal term** $\bar{a}\cos(\omega t) + \bar{b}\sin(\omega t)$.
- $a(t)$ and $b(t)$ are modeled by a full basis of B-splines, forming the **L1-regularized deviation term** $a(t)\cos(\omega t) + b(t)\sin(\omega t)$. Every spline (one per year) has approximately the same scale and support (three years)

Horizontal and vertical **components have separate regularization penalties** due to different observation uncertainties.

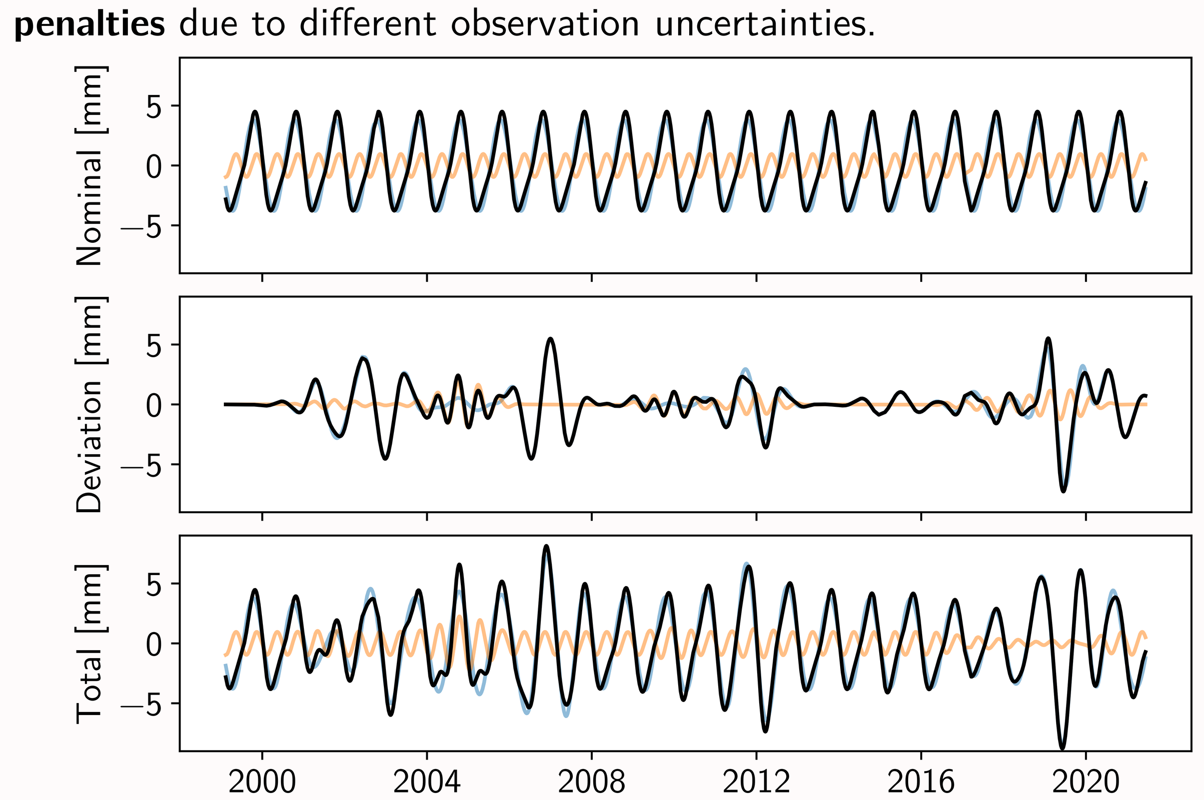

Fig. 6: Seasonal model constituents for station KNOL (see Fig. 4 for location) in the vertical component. The upper two panels show the nominal and deviation terms, respectively, and the bottom panel shows their sum. In each panel, the blue and orange lines correspond to the annual and biannual frequencies, respectively, and the black line is their sum. The overall model is able to adapt well to yearly variations (compare Silverii et al., 2020).

References

- Agrawal, A., Verschueren, R., Diamond, S., & Boyd, S. (2018). A rewriting system for convex optimization problems. Journal of Control and Decision, 5(1), 42–60. https://doi.org/10.1080/23307706.2017.1397554
- Blewitt, G., Hammond, W., & Kreemer, C. (2018). Harnessing the GPS Data Explosion for Interdisciplinary Science. Eos, 99.
- Candès, E. J., Wakin, M. B., & Boyd, S. P. (2008). Enhancing Sparsity by Reweighted ℓ1 Minimization. Journal of Fourier Analysis and Applications, 14(5), 877–905.
- Diamond, S., & Boyd, S. (2016). CVXPY: A Python-Embedded Modeling Language for Convex Optimization. Journal of Machine Learning Research: JMLR, 17, 83.
- Ji, K. H., Herring, T. A., & Llenos, A. L. (2013). Near real-time monitoring of volcanic surface deformation from GPS measurements at Long Valley Caldera, California. Geophysical Research Letters, 40(6), 1054–1058.
- Montgomery-Brown, E. K., Wicks, C. W., Cervelli, P. F., Langbein, J. O., Svarc, J. L., Shelly, D. R., et al. (2015). Renewed inflation of Long Valley Caldera, California (2011 to 2014). Geophysical Research Letters, 42(13), 5250–5257.
- Riel, B., Simons, M., Agram, P., & Zhan, Z. (2014). Detecting transient signals in geodetic time series using sparse estimation techniques. Journal of Geophysical Research: Solid Earth, 119(6), 5140–5160.
- Silverii, F., Montgomery-Brown, E. K., Borsa, A. A., & Barbour, A. J. (2020). Hydrologically Induced Deformation in Long Valley Caldera and Adjacent Sierra Nevada. Journal of Geophysical Research: Solid Earth, 125(5), e2020JB019495.